J Biomol NMR (2012) 52:233–243
DOI 10.1007/s10858-012-9604-y

ARTICLE

Estimating side-chain order in methyl-protonated, perdeuterated proteins via multiple-quantum relaxation violated coherence transfer NMR spectroscopy

Hechao Sun · Raquel Godoy-Ruiz · Vitali Tugarinov

Received: 4 December 2011 / Accepted: 11 January 2012 / Published online: 8 February 2012
© Springer Science+Business Media B.V. 2012

Abstract Relaxation violated coherence transfer NMR spectroscopy (Tugarinov et al. in J Am Chem Soc 129:1743–1750, 2007) is an established experimental tool for quantitative estimation of the amplitudes of side-chain motions in methyl-protonated, highly deuterated proteins. Relaxation violated coherence transfer experiments monitor the build-up of methyl proton multiple-quantum coherences that can be created in magnetically equivalent spin-systems as long as their transverse magnetization components relax with substantially different rates. The rate of this build-up is a reporter of the methyl-bearing side-chain mobility. Although the build-up of multiple-quantum ^{1}H coherences is monitored in these experiments, the decay of the methyl signal during relaxation delays occurs when methyl proton magnetization is in a single-quantum state. We describe a relaxation violated coherence transfer approach where the relaxation of multiple-quantum ^{1}H–^{13}C methyl coherences during the relaxation delay period is quantified. The NMR experiment and the associated fitting procedure that models the time-dependence of the signal build-up, are applicable to the characterization of side-chain order in [$^{13}CH_3$]-methyl-labeled, highly deuterated protein systems up to $\sim$100 kDa in molecular weight. The feasibility of extracting reliable measures of side-chain order is experimentally verified on methyl-protonated, perdeuterated samples of an 8.5-kDa ubiquitin at 10°C and an 82-kDa Malate Synthase G at 37°C.

H. Sun · R. Godoy-Ruiz · V. Tugarinov (✉)
Department of Chemistry and Biochemistry,
Center for Biomolecular Structure and Organization,
University of Maryland, Biomolecular Sci. Bldg.,
College Park, MD 20742, USA
e-mail: vitali@umd.edu

Keywords Relaxation violated coherence transfer NMR spectroscopy · Methyl labeling on the deuterated background · Methyl three-fold axis order parameters · Magnetically equivalent spin-system

Introduction

Three NMR nuclei can serve as spin probes of mobility of methyl-bearing side-chains on the pico-to-nanosecond time-scale in high-molecular-weight proteins (Sheppard et al. 2010). Although deuterium (^{2}H) remains the most reliable and 'straightforward-to-interpret' spin probe of side-chain dynamics, the sensitivity of ^{2}H relaxation measurements in methyls of either $^{13}CH_2D$ (Tugarinov et al. 2005) or $^{13}CHD_2$ (Tugarinov and Kay 2006a; Tugarinov et al. 2005) variety is several times (typically, 3-to-5-fold) lower than that of relaxation methods targeting carbon (^{13}C) nuclei in $^{13}CHD_2$ methyl groups. On the other hand, the interpretation of ^{13}C spin relaxation rates in terms of motional parameters may be significantly more complex (Godoy-Ruiz et al. 2010; Ishima et al. 1999; Sprangers and Kay 2007; Tugarinov and Kay 2005b). Because ^{13}C relaxation in $^{13}CH_3$ methyls is affected by ^{1}H–^{13}C dipolar cross-correlations (Kay et al. 1992; Kay and Torchia 1991), both ^{2}H and ^{13}C-directed spin relaxation measurements require incorporation of at least one deuteron into methyl sites. Since methyl groups of any type—$^{13}CH_2D$, $^{13}CH_2D$ and $^{13}CH_3$—are commonly incorporated into the side-chains of large proteins via the use of appropriately methyl-labeled biosynthetic precursors or amino-acids (Ayala et al. 2009; Gans et al. 2010; Godoy-Ruiz et al. 2010; Religa et al. 2010; Ruschak and Kay 2010; Ruschak et al. 2010b; Sheppard et al. 2010; Sprangers et al. 2007), thus achieving close to 100% content of the methyl type of interest, the

use of any desired methyl isotopomer requires the preparation of a separate protein sample.

Usually, methyl-[$^{13}CH_3$]-labeled samples are produced at initial stages of any NMR study of a large protein system and used for a variety of applications. This makes the use of the third nuclear spin probe—protons in $^{13}CH_3$ methyl groups—an especially attractive and convenient alternative that obviates the need for additional protein preparations with deuterium-containing methyl groups. Furthermore, the starting sensitivity of ^{1}H-directed relaxation measurements in [$^{13}CH_3$]-methyl-protonated, highly deuterated proteins is higher (Ollerenshaw et al. 2005) due to three-fold degeneracy of protons in $^{13}CH_3$ methyl groups and the methyl-TROSY effect (Tugarinov et al. 2003).

Two experimental approaches towards the use of ^{1}H relaxation in $^{13}CH_3$ spin-systems were described previously: (1) the measurement of transverse relaxation rates of individual ^{1}H transitions and extraction of methyl three-fold axis order parameters, S^2_{axis}, that report on the amplitudes of side-chain motions, from the difference in the measured rates (Tugarinov and Kay 2006b), and (2) the more versatile scheme that relies upon the measurement of ^{1}H–^{1}H dipolar cross-correlation rates, η_{HH}, via what was termed as "forbidden fruits of NMR spectroscopy" by Ernst et al. (1987)—namely, the use of relaxation violated coherence transfer (Kay and Prestegard 1987; Muller et al. 1987) whereby methyl proton multiple-quantum (MQ)—so-called 'forbidden'—coherences are created despite that all ^{1}H transitions in a $^{13}CH_3$ methyl are magnetically equivalent. It has been demonstrated that the time dependence of the preparation of ^{1}H MQ states is a sensitive probe of side-chain dynamics, even in systems with molecular weights of hundreds of kilodaltons, and that robust measures of motion can be obtained (Tugarinov et al. 2007). Over the course of several years, the relaxation violated coherence transfer experiment has found applications in the studies of dynamics at methyl sites of a number of large macromolecular assemblies (Kay 2011; Religa et al. 2010; Ruschak et al. 2010a; Sprangers and Kay 2007; Sprangers et al. 2007; Tugarinov et al. 2007). Recently, it has been realized that the selection of triple-quantum (3Q) 'forbidden' proton transitions in the relaxation violated coherence transfer scheme as opposed to the commonly employed double-quantum (2Q) filtering leads to sensitivity gains of 50% (Sun et al. 2011).

Although the main information content of the relaxation violated coherence transfer scheme is provided by the time-dependence of the build-up of MQ ^{1}H magnetization, the decay of the methyl signal during relaxation delays occurs when methyl ^{1}H magnetization is in a single-quantum (SQ) state. Here we describe a 3Q-filtered relaxation violated coherence transfer approach where relaxation of MQ ^{1}H–^{13}C methyl coherences during the relaxation period is measured instead, providing the sum of methyl ^{1}H–^{1}H and ^{1}H–^{13}C cross-correlated relaxation rates, η'. Although not as versatile as the original scheme (Sun et al. 2011), this experiment and the associated modeling of the time-dependence of the methyl signal build-up are applicable to the characterization of side-chain ordering in [$^{13}CH_3$]-methyl-labeled, deuterated proteins of molecular weights up to $\sim$100 kDa. We experimentally verify the feasibility of extracting reliable measures of side-chain order from the rates η' on the samples of {U-[^{15}N,^{2}H]; Ile$^{\delta1}$-[$^{13}CH_3$]; Leu,Val-[$^{13}CH_3$,$^{12}CD_3$]}-ubiquitin (8.5 kDa) at 10°C and {U-[^{15}N,^{2}H]; Ile$^{\delta1}$-[$^{13}CH_3$]}-labeled Malate Synthase G (MSG; 82 kDa; Howard et al. 2000; Tugarinov et al. 2002) at 37°C.

Materials and methods

NMR samples

Two protein samples have been used in this study: (1) {U-[^{15}N,^{2}H]; Ile$^{\delta1}$-[$^{13}CH_3$]; Leu,Val-[$^{13}CH_3$,$^{12}CD_3$]}-labeled human ubiquitin, and (2) {U-[^{15}N,^{2}H]; Ile$^{\delta1}$-[$^{13}CH_3$]}-labeled MSG. All the samples were prepared as described in detail previously (Tugarinov and Kay 2004b) using {U-[^{2}H]}-glucose as the main carbon source and the appropriate α-ketoacid precursors for selective methyl labeling (Tugarinov et al. 2004a; Tugarinov and Kay 2005a). Sample conditions were: 1.2 mM protein concentration, 99.9% D_2O, 25 mM sodium phosphate, pD = 6.8 (uncorrected), 0.05% NaN_3 for ubiquitin; 0.75 mM protein concentration, 99.9% D_2O, 25 mM sodium phosphate, pD = 7.1 (uncorrected), 20 mM $MgCl_2$, 0.05% NaN_3, 5 mM DTT, and a cocktail of protease inhibitors for MSG.

NMR experiments and data analysis

All NMR experiments were conducted at 600 MHz Bruker Avance III spectrometer using a room-temperature triple-resonance probe operating at 10°C (ubiquitin) and 37°C (MSG). All NMR spectra were processed and analyzed using the NMRPipe/NMRDraw suite of programs and associated software (Delaglio et al. 1995). The sum of dipole-dipole ^{1}H–^{1}H and ^{1}H–^{13}C cross-correlated relaxation rates in $^{13}CH_3$ methyl groups, η', has been obtained by fitting the ratios of peak intensities measured in a pair of data sets recorded for each T value ($|I_a/I_b|$) to the functional forms of signal build-up described in the text. Errors in the extracted values of η' were estimated by a Monte-Carlo analysis (Kamith and Shriver 1989) using random noise in the spectra as an estimate of experimental uncertainties in the $|I_a/I_b|$ ratios.

For the measurements of η' the relaxation delays T of (0; 4; 8; 12; 16; 20; 24; 28, 32; 36; 40; 44) ms for ubiquitin, and (0;

0.6; 1.2; 1.8; 2.4; 3.0; 3.6; 4.2; 4.8; 5.3; 6.0) ms for MSG were used. The first point of the $|I_a/I_b|$ build-ups ($T = 0$) for both proteins was measured in a separate experiment with twice more transients and used to calculate the initial conditions in η' measurements (factor f; see text). All the measurements have been performed in the interleaved mode: for the same value of the relaxation delay T and t_1 evolution time the 'allowed' point (intensity I_b) has been acquired immediately after the 'forbidden' one (intensity I_a). Typically, the use of recovery delay of 1.5 s and 24 scans/fid resulted in the net acquisition time of ~4 h. per the pair of 'forbidden' and 'allowed' data sets. For η' measurements in {Ile$^{\delta 1}$-[^{13}CH$_3$]}-MSG, 48 scans/fid and 1.0 s recovery delay resulted in ~6 h. per pair of experiments.

Extraction of methyl three-fold axis order parameters, S^2_{axis}, from relaxation data requires the knowledge of the overall molecular tumbling time (τ_C). The correlation time of ubiquitin (D_2O; 10°C) determined previously in H_2O at 10°C from ^{15}N relaxation data (Sheppard et al. 2009) has been scaled by the ratio of D_2O/H_2O viscosities at 10°C (Cho et al. 1999), τ_C (D_2O) = $[\eta^{D_2O}/\eta^{H_2O}]\tau_C$ (H_2O), leading to the isotropic τ_C value of 8.9 ns. The values of the diffusion tensor for MSG (D_2O; 37°C) were estimated from diffusion measurements as described previously (Tugarinov and Kay 2006b; Tugarinov et al. 2005) resulting in $\tau_{C,\text{eff}} = (2D_{||} + 4D_{\perp})^{-1} = 49$ ns, diffusion anisotropy $D_{||}/D_{\perp} = 1.21$ and the polar angles $\theta = 13°$, $\phi = 48°$ defining the orientation of the unique diffusion axis relative to the inertia frame (Tugarinov and Kay 2006b).

Results and discussion

The background on relaxation violated coherence transfer NMR experiments for estimation of side-chain order in methyl-protonated, highly deuterated large proteins

Relaxation violated coherence transfer NMR experiments that have been developed earlier (Sun et al. 2011; Tugarinov et al. 2007) for quantification of side-chain order in large proteins selectively labeled with ^{13}CH$_3$ methyl groups on the deuterated background, are better understood with reference to the energy level diagram of an AX$_3$ (^{13}CH$_3$) spin-system shown in Fig. 1. For an 'isolated' methyl group attached to a macromolecule and assuming very rapid methyl rotation about its three-fold axis, the relaxation rates of each of the ^{1}H SQ transitions is single-exponential in the macromolecular limit, with fast ($R^F_{2,H}$; shown with cyan and black vertical arrows connecting proton states |1> and |2>, |3> and |4> in Fig. 1) or slow ($R^S_{2,H}$; red vertical arrows; Fig. 1) rates (Kay and Prestegard 1987; Muller et al. 1987; Tugarinov et al. 2003). It has also been demonstrated that under these assumptions each of the ^{1}H–^{13}C MQ, double-(DQ)-/zero-(ZQ)-quantum, coherences decays in a single-exponential manner with fast ($R^F_{\text{DQ}}, R^F_{\text{ZQ}}$; shown with blue diagonal arrows in Fig. 1) or slow ($R^S_{\text{DQ}}, R^S_{\text{ZQ}}$; red diagonal arrows; Fig. 1) rates (Tugarinov et al. 2003). The relaxation violated coherence transfer scheme developed previously (Sun et al.

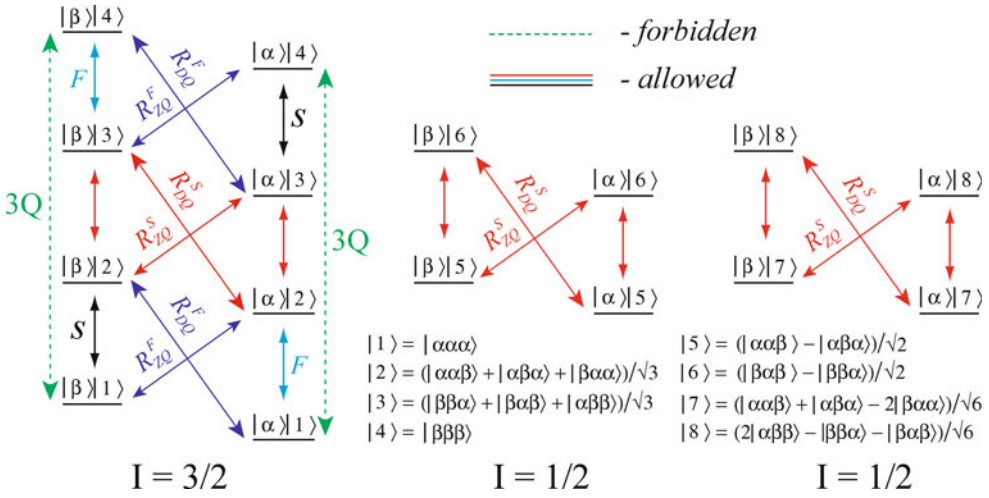

Fig. 1 Energy level diagram for the AX$_3$ spin-system of a ^{13}CH$_3$ methyl group. Eigenfunctions are denoted by |*i*> |*n*> where *i* and *n* refer to the ^{13}C and ^{1}H spin states, respectively ($i \in \{\alpha,\beta\}$ and |*n*> ≡ |*j,k,l*>, where (j,k,l) $\in \{\alpha,\beta\}$). All 'allowed' transitions are shown with *solid arrows*. *Vertical solid arrows* correspond to ^{1}H SQ transitions, while ^{1}H–^{13}C double-quantum (DQ) and zero-quantum (ZQ) slow (*fast*)-relaxing transitions are shown with *red* (*blue*) *diagonal arrows* and labeled $R^S_{\text{DQ/ZQ}}\left(R^F_{\text{DQ/ZQ}}\right)$. Triple-quantum 'forbidden' ^{1}H transitions are shown with *dashed green arrows* and labeled '3Q'. The slow-relaxing SQ ^{1}H transitions are shown with *red vertical arrows*, while the fast-relaxing ^{1}H transitions connecting levels |1> and |2>, |3> and |4>, are differentiated onto two types—those that relax faster due to C–H/H–H dipole-dipole cross-correlated spin relaxation (labeled with '*F*' and shown with *cyan vertical arrows*) and those that relax slower (labeled with '*S*' and shown with *black vertical arrows*)

2011; Tugarinov et al. 2007) quantifies the cross-correlated relaxation rates between the pairs of ^{1}H–^{1}H vectors in a $^{13}CH_3$ methyl group, η_{HH}. In the macromolecular limit, $\eta_{HH} = \left(R^{F}_{2,H} - -R^{S}_{2,H}\right)/2$, and is directly related to the amplitude of motions of the methyl three-fold axis expressed as a generalized order parameter, S^2_{axis} (Lipari and Szabo 1982). As long as $\eta_{HH} \neq 0$, i.e. a substantial difference exists between the relaxation rates of the fast- and slow-relaxing ^{1}H transitions in a $^{13}CH_3$ spin-system, experiments are designed that exploit the relaxation violated coherence transfer whereby methyl proton MQ coherences—for example, 3Q transitions shown with dashed green vertical arrows in Fig. 1—can be prepared despite that all ^{1}H transitions in $^{13}CH_3$ groups are magnetically equivalent. In the absence of differential relaxation ($\eta_{HH} = 0$), these transitions are 'forbidden' and cannot be excited (Ernst et al. 1987; Kay and Prestegard 1987; Müller et al. 1987).

Two experiments are performed: (*a*) with selection of 'forbidden' MQ ^{1}H transitions leading to the time dependence of the signal intensities I_a in the form $I_a(t) = A\sinh(\eta_{HH}t)$ (we assume for simplicity an isolated methyl that has no interactions with external proton spins), and (*b*) with selection of SQ ^{1}H transitions leading to a bi-exponential decay of signal intensities $I_b(t) = B\cosh(\eta_{HH}t)$. For an isolated methyl group, the time-dependence of the ratio of intensities in these two experiments $|I_a/I_b|(t) = (A/B)\tanh(\eta_{HH}t)$ can be used to extract the estimates of η_{HH} and hence S^2_{axis}. The magnitude of the 'pre-factor' A/B above depends upon the relative efficiencies of magnetization transfer in the two experiments and the order of MQ proton coherences selected in experiment *a*. In practice, however, even in highly deuterated proteins methyl groups are not isolated; rather they interact with other protonated methyls in protein structures, and the $|I_a/I_b|$ ratios are fitted to a more complex relationship that models the 'build-up' of $|I_a/I_b|$ as a function of time taking into account cross-relaxation between the slow- and fast-relaxing transitions induced by dipolar interactions with external ^{1}H spins (Tugarinov et al. 2007). The time dependence of such a build-up has been shown to provide a sensitive and reliable probe of methyl-axis dynamics, even in proteins the size of 360-kDa $\alpha_7\alpha_7$ 'half-proteasome' construct (Tugarinov et al. 2007). Although in the original version of the relaxation violated transfer scheme 2Q 'forbidden' proton coherences were selected in experiment *a*, it has been shown recently that the sensitivity of the experiment benefits significantly (by a factor of 3/2) from the selection of 3Q 'forbidden' proton magnetization (Sun et al. 2011). Keeping this 50% increase in sensitivity provided by 3Q-filtering of the 'forbidden' magnetization in mind, we explore the feasibility of estimation of S^2_{axis} via the measurement of the sum of ^{1}H–^{1}H and ^{1}H–^{13}C cross correlated relaxation rates in $^{13}CH_3$ methyls of highly deuterated proteins, $\eta' = \eta_{HH} + \eta_{CH}$, using a MQ version of the 3Q-selected relaxation violated coherence transfer.

Measurements of the sum of ^{1}H–^{1}H and ^{1}H–^{13}C cross-correlated relaxation rates in methyl groups via relaxation violated coherence transfer

Figure 2 shows the relaxation violated coherence transfer scheme which monitors the evolution of methyl ^{1}H–^{13}C MQ magnetization during the relaxation period *T*. The 90° $^{13}C_{\phi 2}$ pulse applied at time-point *a* of the scheme (Fig. 2) converts methyl ^{1}H SQ magnetization to a superposition of DQ and ZQ coherences. The fast-$\left(R^{F}_{DQ}; R^{F}_{ZQ}\right)$ and slow-$\left(R^{F}_{DQ}; R^{F}_{ZQ}\right)$ relaxing MQ magnetization evolves during the relaxation delay *T*, and is subsequently converted back to the ^{1}H SQ state anti-phase with respect to the methyl carbon spin by the ^{13}C 90° pulse at time-point *b*. As in the case of previous SQ ^{1}H relaxation-based measurements (Sun et al. 2011; Tugarinov et al. 2007), two experiments are performed: (*a*) the first experiment with the 'open' $^{1}H_{\phi 4}$ pulse included in Fig. 2 selecting for 'forbidden' 3Q ^{1}H transitions (dashed green arrows in Fig. 1); the build-up of the 3Q-filtered 'forbidden' magnetization leads to correlations with intensities I_a, and (*b*) the second experiment performed with the 'open' $^{1}H_{\phi 4}$ pulse omitted selecting for ^{1}H SQ ('allowed') transitions providing intensities I_b. In the rest of the scheme, the magnetization is converted back to the MQ state and 'filtered' between time-points *c* and *d* (Fig. 2) to eliminate the 'fast' MQ transitions (blue diagonal arrows in Fig. 1) so that only the 'slow' part of the $I = 3/2$ manifold (Fig. 1) in the 'forbidden' experiment and the 'slow' parts of all manifolds in the 'allowed' experiment evolve during the t_1 period (Korzhnev et al. 2004; Sheppard et al. 2010). As described in detail below, the time-dependence of the experimental ratio $|I_a/I_b|$ is modeled with the purpose of reliable extraction of order parameters S^2_{axis} taking into account that the 'fast' and the 'slow' parts of the MQ ^{1}H–^{13}C magnetization relaxing during *T* do not evolve independently and are coupled due to interactions with external proton spins. Detailed analyses of the magnetization transfer pathways in experiments *a* and *b* for the case when the time evolution of SQ ^{1}H transitions is monitored during *T* can be found in the previous publications (Sun et al. 2011; Tugarinov et al. 2007).

The relaxation rates of the DQ and ZQ parts are very different for both the fast-$\left(R^{F}_{DQ}; R^{F}_{ZQ}\right)$ and slow-$\left(R^{S}_{DQ}; R^{S}_{ZQ}\right)$ relaxing transitions (Tugarinov and Kay 2004a; Tugarinov et al. 2004b). However, the DQ and ZQ rates are effectively averaged by the application of ^{1}H and

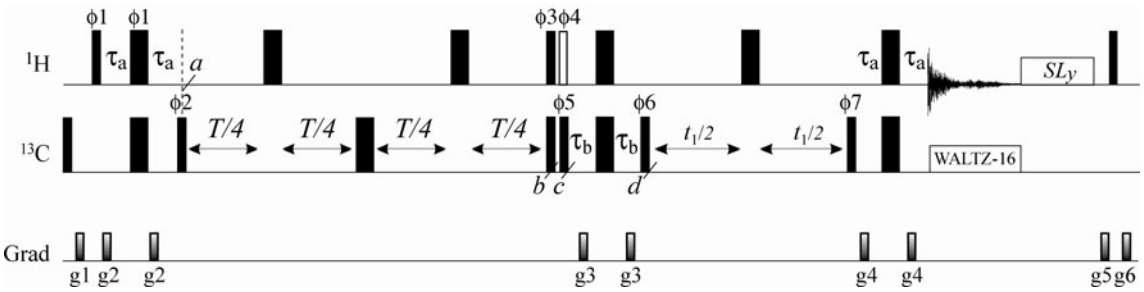

Fig. 2 The pulse scheme for the measurement of intra-methyl ^{1}H–^{1}H + ^{1}H–^{13}C dipole-dipole cross-correlated spin relaxation rates, η', in $^{13}CH_3$ groups of perdeuterated proteins. The scheme with the open ^{1}H pulse (phase $\phi4$) included at point *b* is used to measure the build-up of ^{1}H 3Q coherences during the relaxation delay T (resulting in correlations with intensities I_a), while a second experiment is recorded to measure the bi-exponential decay of ^{1}H–^{13}C MQ magnetization by removing the open pulse (correlations with intensities I_b). All narrow (wide) rectangular pulses are applied with flip angles of 90(180)° along the *x*-axis unless indicated otherwise. The ^{1}H carrier is positioned in the center of the Ile$^{\delta1}$-Leu-Val methyl region (0.7 ppm), while the ^{13}C carrier is positioned at 12(19) ppm for Ile$^{\delta1}$(ILV)-labeled samples. All ^{1}H and ^{13}C pulses are applied with the highest possible power, with WALTZ-16 (Shaka et al. 1983) ^{13}C decoupling achieved using a 2-kHz field. A 40 ms ^{1}H spin-lock (8 kHz, *y*-axis) is applied after acquisition ('SLy'). The spin-lock pulse and the subsequent ^{1}H purge pulses eliminate all transverse components of ^{1}H magnetization before the recovery delay. Delays are: $\tau_a = 1/(4^1J_{CH}) = 2.0$ ms; $\tau_b = 1/(8^1J_{CH}) = 1$ ms; T is the variable relaxation delay. The phase cycle is: $\phi1 = (0°,60°,120°,180°,240°,300°)$; $\phi2 = 3(x),3(-x)$; $\phi3 = \phi1$; $\phi4 = 6(x),6(-x)$; $\phi5 = 12(x),12(-x)$; $\phi6 = 6(y),6(-y)$; $\phi7 = x$; rec. $= 4(x,-x,x),4(-x,x,-x)$ (3Q-filtered 'forbidden' experiment with the open $^1H_{\phi4}$ pulse included), and $\phi1 = x,-x$; $\phi2 = \phi3 = 3(x),3(-x)$; $\phi5 = 12(x),12(-x)$; $\phi6 = 6(y),6(-y)$; $\phi7 = x$; rec. $= 4(x,-x,x),4(-x,x,-x)$ (the 'allowed' experiment; open $^1H_{\phi4}$ pulse omitted). The durations and strengths of pulsed-field *z*-gradients in units of (ms; G/cm) are: g1 = (1; 5), g2 = (0.05; −20), g3 = (0.5; 10), g4 = (0.15; 12), g5 = (1.0; 10), g6 = (1.2; 8). Quadrature detection in F_1 is achieved via STATES-TPPI (Marion et al. 1989) incrementation of $\phi7$

^{13}C 180° pulses during T that eliminate contributions from intra-methyl H–H/C–H cross-correlated relaxation as well as from cross-correlations involving external protons and deuterons. In what follows, we therefore denote $\left(R^F_{DQ} + R^F_{ZQ}\right)/2$ by R^F_{MQ} and $\left(R^S_{DQ} + R^S_{ZQ}\right)/2$ by R^S_{MQ}. The relaxation of the lines of the methyl MQ multiplet (L_1 through L_4) during the delay T in the presence of dipolar interactions with external proton spins can be then described by (Korzhnev et al. 2004; Tugarinov et al. 2007):

$$\frac{d}{dT}\begin{pmatrix} L_1 - L_3 \\ L_2 \\ L_1 + L_3 \\ L_4 \end{pmatrix} = -\left\{ \begin{array}{c} \mathrm{diag}[R^F_{MQ}; R^S_{MQ}; R^F_{MQ}; R^S_{MQ}] + \\ k_{HH}\begin{bmatrix} 9 & 0 & 0 & 0 \\ 0 & 9 & -4 & 2\sqrt{2} \\ 0 & -4 & 9 & -2\sqrt{2} \\ 0 & 2\sqrt{2} & -2\sqrt{2} & 7 \end{bmatrix} \end{array} \right\} \times \begin{pmatrix} L_1 - L_3 \\ L_2 \\ L_1 + L_3 \\ L_4 \end{pmatrix} \quad (1)$$

where $(L_1{-}L_3; L_2; L_1 + L_3; L_4) = 2C_{tr}\left(\frac{\rho_{34}-\rho_{12}}{\sqrt{2}}; \frac{2\rho_{23}+\rho_{56}+\rho_{78}}{\sqrt{6}}; \frac{\rho_{34}+\rho_{12}}{\sqrt{2}}; \frac{\rho_{23}-\rho_{56}-\rho_{78}}{\sqrt{3}}\right)$, C_{tr} is the spin operator of transverse ^{13}C magnetization ($C_{x,y}$), ρ_{kl} is the density element coupling the proton states |k> and |l> (Fig. 1), and $k_{HH} = \sum_{ext}\left(\frac{1}{20}\right)\frac{\hbar^2\gamma_H^4\tau_C}{r^6_{HHext}}$, where r_{HHext} are the distances to external proton nuclei, and the sum runs over all external proton spins. The build-up of the ratio of intensities obtained in the two experiments, $|I_a/I_b|$, will be determined by the sum of intra-methyl ^{1}H–^{1}H and ^{1}H–^{13}C dipole-dipole cross-correlation rates, η', that in the macromolecular limit is given by

$$\begin{aligned} \eta' = \eta_{HH} + \eta_{CH} &= \frac{R^F_{MQ} - R^S_{MQ}}{2} \\ &\approx S^2_{axis}\gamma^2_H\hbar^2\tau_C\left(\frac{\mu_0}{4\pi}\right)^2\left\{\frac{9}{10}\left[P_2(\cos\theta_{axis,HH})\right]^2\frac{\gamma^2_H}{r^6_{HH}}\right. \\ &\left. + \frac{2}{5}\left[P_2(\cos\theta_{axis,CH})\right]^2\frac{\gamma^2_C}{r^6_{CH}}\right\} \end{aligned} \quad (2)$$

where τ_C is the global molecular tumbling time, μ_0 is the vacuum permeability constant, γ_i is the gyromagnetic ratio of spin i, r_{HH} is the distance between pairs of methyl protons, r_{CH} is the distance between the carbon and proton nuclei, $P_2(x) = \frac{1}{2}(3x^2 - 1)$, and $\theta_{axis,HH}$ is the angle between the methyl three-fold axis and a vector that connects a pair of methyl ^{1}H nuclei, while $\theta_{axis,CH}$ is the angle between the methyl three-fold axis and a vector that connects ^{13}C and ^{1}H nuclei. Assuming ideal tetrahedral methyl geometry ($\theta_{axis,CH} = 109.5°$; $r_{CH} = 1.135$ Å; Mittermaier and Kay 2002; Ottiger and Bax 1999) and $r_{HH} = 1.813$ Å (Ishima et al. 2001; Tugarinov et al. 2006), we calculate that $\eta_{HH} + \eta_{CH} = 1.21\eta_{HH}$, i.e. ^{1}H–^{13}C cross-correlations contribute a relatively small portion of the total cross-correlated relaxation rate that is responsible for the narrowing of central, slowly-relaxing lines in methyl-TROSY spectroscopy

(Tugarinov et al. 2003; i.e. $R^S_{MQ} \approx 0$ for an isolated methyl group (Tugarinov et al. 2003), and the line-widths of central MQ transitions are largely determined by dipolar interactions with external protons and deuterons). Of note, the same value of $r_{HH} = 1.813$ Å has been used in earlier methyl ^{1}H relaxation studies (Sun et al. 2011; Tugarinov and Kay 2006b; Tugarinov et al. 2007) and is in reasonable agreement with the value of 1.807 ± 0.012 Å reported for methyl iodide based on the ratios of methyl ^{1}H–^{1}H and ^{1}H–^{13}C dipolar couplings (Wooten et al. 1979), while the chosen value of r_{CH} corresponds to $\langle P_2(\cos\theta_{axis,CH}) r_{CH}^{-3} \rangle = -0.228$ Å^{-3} assuming ideal methyl tetrahedrality ($\theta_{axis,CH} = 109.5°$) as derived from the ratios ^{13}C–^{13}C$_m$ and ^{1}H–^{13}C dipolar couplings in a pair of previous studies (Mittermaier and Kay 2002; Ottiger and Bax 1999).

The modeling of the time-dependence of the $|I_a/I_b|$ build-up in the experiment of Fig. 2 is somewhat more involved than in the previous ^{1}H SQ relaxation-based scheme(s). The principal difficulty is associated with the determination of initial conditions for solution of the system of differential equations (1), namely the relative amount of 'fast' and 'slow' magnetization present at time-point *a* of the scheme in Fig. 2. Apart from ^{1}H–^{1}H cross-correlations that are operative during the initial delay $2\tau_a$, cross-correlated relaxation between ^{1}H–^{1}H and ^{1}H–^{13}C dipoles in a methyl group ($\eta_{HH/CH}$) will affect the intensities of the fast-relaxing part of ^{1}H SQ coherences evolving till the time-point *a* of the scheme. These cross-correlations lead to different relaxation rates of the 'fast' ^{1}H SQ transitions depending on the state of the carbon spin as it is shown in Fig. 1, where ^{1}H SQ transitions associated with ^{13}C spin states $|\alpha\rangle$ or $|\beta\rangle$ are separated onto those that relax faster due to H–H/C–H cross-correlated relaxation ($+\eta_{HH/CH}$; labeled with '*F*' in Fig. 1) and those that decay slower ($-\eta_{HH/CH}$; labeled with '*S*'). The rates $\eta_{HH/CH}$ are significant: in the macromolecular limit, and for standard methyl geometry, $\eta_{HH/CH}$ is equal to $\frac{1}{5}\left(\frac{\mu_0}{4\pi}\right)^2 \frac{2S^2_{axis}\gamma_H^3\gamma_C\hbar^2\tau_C}{r_{HH}^3 r_{CH}^3}$ which amounts to approximately 8/9 of the ^{1}H–^{1}H cross-correlated relaxation rates η_{HH}. Of note, the same type of cross-correlations differentiates the relaxation rates of proton transitions in fast-rotating ^{13}CH$_2$(D) methyl groups, and has been utilized earlier in ^{13}CH$_2$(D)-methyl TROSY-based experiments (Tugarinov and Kay 2006b; Tugarinov et al. 2005). In small proteins, the cross-correlated relaxation rates $\eta_{HH/CH}$ can be measured using modifications of the pulse-schemes developed earlier for isolation and relaxation rate measurements of linear combinations of 'fast' ($\rho_{1-2} + \rho_{3-4}$; $\rho_{1-2} - \rho_{3-4}$) and 'slow' ($2\rho_{2-3} + \rho_{5-6} + \rho_{6-7}$) ^{1}H transitions (Tugarinov and Kay 2006b). In Fig. 3 we show a pair of examples of relaxation decay curves of the 'fast' ^{1}H SQ transitions corresponding to different methyl ^{13}C spin states (α/β) recorded in ubiquitin at 27°C. Clearly, the differences in decay rates of the two 'fast' ^{1}H transitions corresponding to $^{13}C^{\alpha}$ or $^{13}C^{\beta}$ states are substantial complicating the determination of initial conditions for solution of (1). Note that the effects of cross-correlations involving methyl ^{1}H CSA—such as between methyl ^{1}H CSA and ^{1}H–^{1}H or ^{1}H–^{13}C dipoles—are eliminated by application of 180° ^{1}H and ^{13}C pulses during the first delay $2\tau_a$ in the scheme of Fig. 2.

Because taking into account accurately the evolution of the 'fast' SQ ^{1}H transitions during the initial delay $2\tau_a$ in the presence of H–H/C–H cross-correlations and external proton spins is not straightforward, we have chosen to use the following simple procedure that boils down to 'fixing' the first point of the $|I_a/I_b|$ build-up to its experimentally measured value at $T = 0$ (time-point *a* in Fig. 2). As the 'fast' and 'slow' magnetization pathways are not intermixed by the application of the $^{13}C_{\phi 2}$ pulse (Ollerenshaw et al. 2003; Tugarinov et al. 2003), the time-dependence of $|I_a/I_b|$ can be expressed as,

$$\left|\frac{I_a}{I_b}\right|(T) = -\frac{3}{4}\left\{\frac{F_a F_{MQ}(T) - S_a S_{MQ}(T)}{F_a F_{MQ}(T) + S_a S_{MQ}(T)}\right\} \quad (3)$$

where S_a (F_a) is the amount of 'slow'('fast') magnetization (signal intensity) at time-point *a* of the scheme, and S_{MQ} (F_{MQ}) is the time-dependent MQ 'slow'('fast')

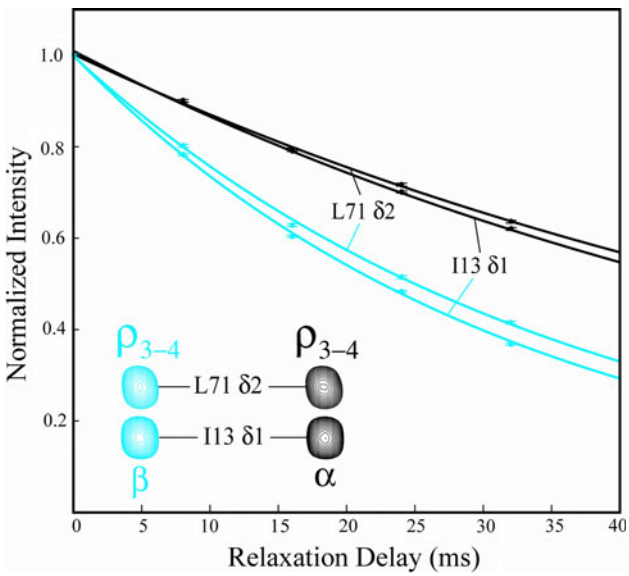

Fig. 3 Examples of relaxation decay curves of the 'fast' group of ^{1}H SQ transitions for a pair of selected methyl positions in ubiquitin (27°C). The color coding is the same as in the diagram of Fig. 1. For the case of ^{1}H SQ transitions connecting levels |3> and |4> in the diagram of Fig. 1 (ρ_{3-4}), the transitions that relax slower due to H–H/C–H dipole-dipole cross-correlations correspond to the ^{13}C spin-state α (shown in *black*), while those that correspond to the ^{13}C spin-state β relax faster (shown in *cyan*). The opposite is true for the ^{1}H SQ transitions connecting levels |1> and |2> in Fig. 1

magnetization. At $T = 0$, $|I_a/I_b|(0) = (-3/4)(F_a - S_a)/(F_a + S_a)$. The pre-factor of $(-3/4)$ in (3) derives from the calculation of the relative efficiencies of 'forbidden' and 'allowed' magnetization transfers in the case of 3Q selection as described in detail previously (Sun et al. 2011), and assumes that an equal number of scans is acquired in the 'forbidden' (I_a) and 'allowed' (I_b) experiments. We define the ratio $f = S_a/F_a$ and calculate from (3) at $T = 0$:

$$f = \frac{1 + (4/3)\left|\frac{I_a}{I_b}(0)\right|}{1 - (4/3)\left|\frac{I_a}{I_b}(0)\right|} \tag{4}$$

Experimental determination of the factor f thus allows defining the appropriate initial conditions for modeling of the time-dependence of $|I_a/I_b|$ build-up. For more accurate determination of f, the first point of the experiment in Fig. 2 ($T = 0$) can be collected with more scans (see "Materials and methods"). The subsequent modeling of $|I_a/I_b|(T)$ closely follows the analysis in Tugarinov et al. (2007). Noting that initial conditions for solution of (1) may be approximated by $\left(0, \frac{\sqrt{6}}{2}, \frac{\sqrt{6}}{2f}, 0\right)$ and assuming that $2C_{\rm tr}\rho_{23}(T) = 2C_{\rm tr}[\rho_{56}(T) + \rho_{78}(T)]$ for all T, the time dependence of the terms of interest may be approximated by:

$$\frac{d\vec{v}(T)}{dT} = -\tilde{M}\vec{v}(T) \tag{5a}$$

where

$$\vec{v}^T = 2C_{\rm tr}\left[\frac{(2\rho_{23} + \rho_{56} + \rho_{78})}{\sqrt{6}}, \frac{(\rho_{34} + \rho_{12})}{\sqrt{2}}\right] \tag{5b}$$

$$\tilde{M} = \begin{pmatrix} R^S_{\rm MQ} + R_{\rm ext} & \delta \\ \delta & R^F_{\rm MQ} + R_{\rm ext} \end{pmatrix} \tag{5c}$$

and $R_{\rm ext} = 9k_{\rm HH}$, $\delta = -4k_{\rm HH}$. We note that the magnitude of L_4 in (1) at $T = 0$ is not exactly zero. Simulations show, however, that the build-up of L_4 during the delay $2\tau_a$ is negligibly small even for large proteins. Solution of the system of differential equations (5a) under the initial conditions specified above yields the following expression for the time-dependence of $|I_a/I_b|$,

$$\left|\frac{I_a}{I_b}\right|(T) = -\frac{3}{4}\left\{\frac{F_{\rm MQ}(T) - f\,S_{\rm MQ}(T)}{F_{\rm MQ}(T) + f\,S_{\rm MQ}(T)}\right\} \tag{6a}$$

where

$$F_{\rm MQ} = \cosh(\sigma' T) - \left[\frac{\eta' + f\delta}{\sigma'}\right]\sinh(\sigma' T), \tag{6b}$$

$$S_{\rm MQ} = \cosh(\sigma' T) + \left[\frac{f\eta' - \delta}{f\sigma'}\right]\sinh(\sigma' T) \tag{6c}$$

$$\sigma' = \frac{1}{2}\sqrt{4\eta'^2 + 4\delta^2} \tag{6d}$$

and f is determined experimentally using (4). Equation (6a) is used for the two-parameter fitting of the experimental $|I_a/I_b|$ ratios for extraction of η' and δ. The order parameters $S^2_{\rm axis}$ are subsequently calculated from η' rates using (2).

Unlike SQ ^{1}H transitions in a methyl group that are all degenerate, lines L_1 through L_3 of the ^{1}H–^{13}C MQ triplet evolving during the relaxation period T according to (1), are separated by the value of ^{1}H–^{13}C J coupling, $^1J_{\rm CH}$ ($\sim$125 Hz). In the basis set of (1), this translates to the coupling of the fast-relaxing terms $(L_1 - L_3)$ and $(L_1 + L_3)$ by $\pm 2i\pi^1 J_{\rm CH}$. In the derivations above we have been assuming that the ^{1}H and ^{13}C 180° pulses applied during the relaxation delay T completely decouple the lines of the multiplet. This is not the case, however, in the presence of the 'cross-talk' between the lines which is induced by ^{1}H spin-flips and expressed by the parameter $\delta = -4k_{\rm HH}$ in (5c). The evolution of the spin-system under the effect of (residual) J coupling will affect the form of the time-dependence of $|I_a/I_b|$ ratios. The magnitude of this effect will depend on η' and δ, i.e. the molecular tumbling time $\tau_{\rm C}$, $S^2_{\rm axis}$, and the proximity of a given methyl to external proton spins. To assess the extent to which the derived η' (and consequently, $S^2_{\rm axis}$) will be compromised by residual couplings, we have simulated $|I_a/I_b|$ build-ups in the presence of $^1J_{\rm CH}$ coupling during the delay T and fitted the synthetic data to (6a) which implicitly assume complete decoupling. Figure 4 shows the contour plots showing relative deviations of the derived $S^2_{\rm axis}$ (in %), $\left(S^2_{\rm fit} - S^2_{\rm sim}\right)/S^2_{\rm sim}$, where $S^2_{\rm fit}$ is the order parameter derived from the fitted cross-correlation rates η' using (6a) and $S^2_{\rm sim}$ is the order parameter input into the synthetic $|I_a/I_b|$ ratios, for molecular tumbling times $\tau_{\rm C} = 10$ ns (Fig. 4a) and $\tau_{\rm C} = 50$ ns (Fig. 4b). It is clear from Fig. 4a that for proteins approximately the size of ubiquitin at 10°C, the effects of residual J evolution on the extracted $S^2_{\rm axis}$ is predicted to be very small for the whole range of order parameters and distances to external proton spins $r_{\rm HHext}$. Of note, in all simulations, the order parameter of dipolar interactions with external proton spins was assumed to be equal to unity which clearly represents an upper bound on the relaxation contributions of external protons. If the order parameter of external interactions is assumed to be equal to $S^2_{\rm axis}$, much smaller errors are obtained for shorter $r_{\rm HHext}$ distances in Fig. 4a–b. Furthermore, the situation when both $S^2_{\rm axis}$ and $r_{\rm HHext}$ are small ($S^2_{\rm axis} < \sim 0.5$; $r_{\rm HHext} < \sim 3.0$ Å) is hardly realized in practice, as it would imply a disordered side-chain located deep in the hydrophobic core of a protein in immediate proximity to other methyl protons.

The low level of discrepancy in Fig. 4a can be explained by the observation that even though the functional form of

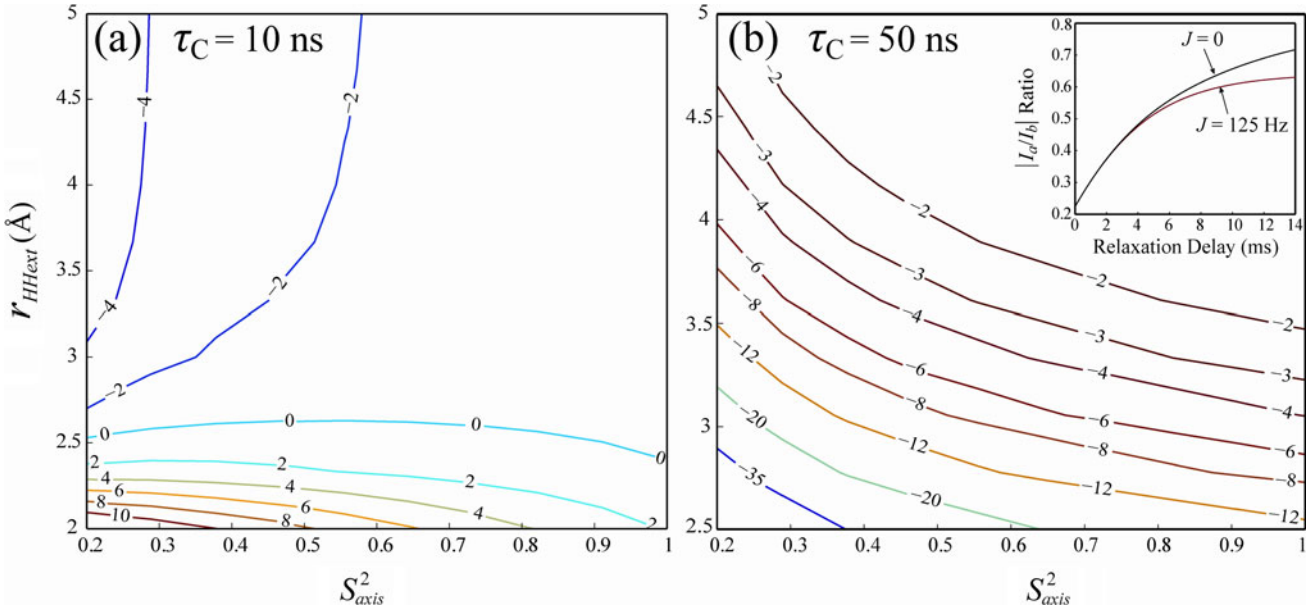

Fig. 4 Contour plots showing relative deviations of S^2_{axis} (in %) obtained from the fit of the simulated $|I_a/I_b|$ build-up to (6a), $100 * \left(S^2_{\text{fit}} - S^2_{\text{sim}}\right)/S^2_{\text{sim}}$ where S^2_{fit} is the order parameter derived from the fitted cross-correlation rates (2) and S^2_{sim} is the order parameter input into the synthetic $|I_a/I_b|$ ratios, as a function of S^2_{axis} (*x*-axis) and the distance (Å) to an external proton spin (r_{HHext}, *y*-axis) for the global molecular reorientation correlation times (τ_C) of (**a**) 10 ns; (**b**) 50 ns. *Errors* (in %) are indicated for each *contour line*. In all calculations, external spins are represented by a single proton located at the effective distance r_{HHext} from the methyl group of interest. The order parameter S^2_{axis} for the dipolar interaction with the external proton spin was set to 1 for all calculations (see text). The inset in **b** shows a theoretical build-up curve of the $|I_a/I_b|$ ratio simulated for a molecule with $\tau_C = 50$ ns in the absence of J ($^1J_{\text{CH}} = 0$; *black curve*) and with $^1J_{\text{CH}} = 125$ Hz (*red curve*), for $S^2_{\text{axis}} = 0.65$ and $r_{\text{HHext}} = 2.3$ Å. Note that the differences between the build-up curves are intentionally exaggerated since the simulation has been performed for a short distance to the external proton spin (2.3 Å), and with the order parameter for the interaction set to 1

the $|I_a/I_b|$ time-dependence is significantly affected by residual J couplings, these differences will be entirely absorbed by the parameter δ, with practically no effect on the extracted η' and hence S^2_{axis}. Further simulations show that this 'fortuitous' scenario would hold for molecular tumbling times up to ~25 ns. For larger molecules such as MSG, simulations in the presence of $^1J_{\text{CH}}$ predict that an underestimate of the derived S^2_{axis} on the order of several percent would result from incomplete decoupling as indicated by the contour plots in Fig. 4b. As discussed above, the simulated errors clearly represent upper-bound estimates as long as the order parameter of interactions with external protons is set to 1. The inset to the figure illustrates the intentionally exaggerated differences between the $|I_a/I_b|$ build-ups in the presence (red curve) and absence (blue curve) of J coupling calculated with r_{HHext} set to the unrealistically low value of 2.3 Å for an Ile$^{\delta 1}$-{^{13}CH$_3$} labeled protein sample. It is clear from the comparison of the curves that the most experimentally straightforward way to avoid the underestimation of η'-derived S^2_{axis} in larger proteins would be the acquisition of *initial* $|I_a/I_b|$ build-up curves, i.e. until the effects of incomplete decoupling are still approximately within the errors in the measurement. For Ile$^{\delta 1}$-{^{13}CH$_3$}-labeled MSG, the $|I_a/I_b|$ build-ups have been therefore recorded for the relaxation delay $T \leq 6$ ms (see "Materials and methods"). We note that a 1-kHz strong CPMG pulse train (Carr and Purcell 1954; Meiboom and Gill 1958) applied on ^{13}C nuclei (Korzhnev et al. 2004) in the experiment of Fig. 2 solves the problem only partially; indeed, further simulations show that for longer relaxation delays T stronger fields are required to completely eliminate the effects of J coupling in the presence of ^{1}H spin-flips.

Experimental verification

Below we describe the results of η' measurements in ubiquitin (10°C) and MSG (37°C). Figure 5a–b show some typical build-up curves of experimental intensity ratios, $|I_a/I_b|$, obtained using the experiment of Fig. 2 for methyl groups of {U-[^{2}H]; Ile$^{\delta 1}$-[^{13}CH$_3$]; Leu,Val-[^{13}CH$_3$,^{12}CD$_3$]}-labeled ubiquitin (5a) and {U-[^{2}H]; Ile$^{\delta 1}$-[^{13}CH$_3$]}-labeled MSG (5b) best-fit to the functional form in (6a). Note that the first point of the fit ($T = 0$) is 'fixed' to its experimental value, and the factor f entering (6a–6d) is calculated using the relationship in (4). The average experimental values of factor f are 1.14(1.82) in ubiquitin (MSG). The average η' rates (±1 standard deviation) of 24.5 ± 7 s^{-1} and 130 ± 34 s^{-1} have

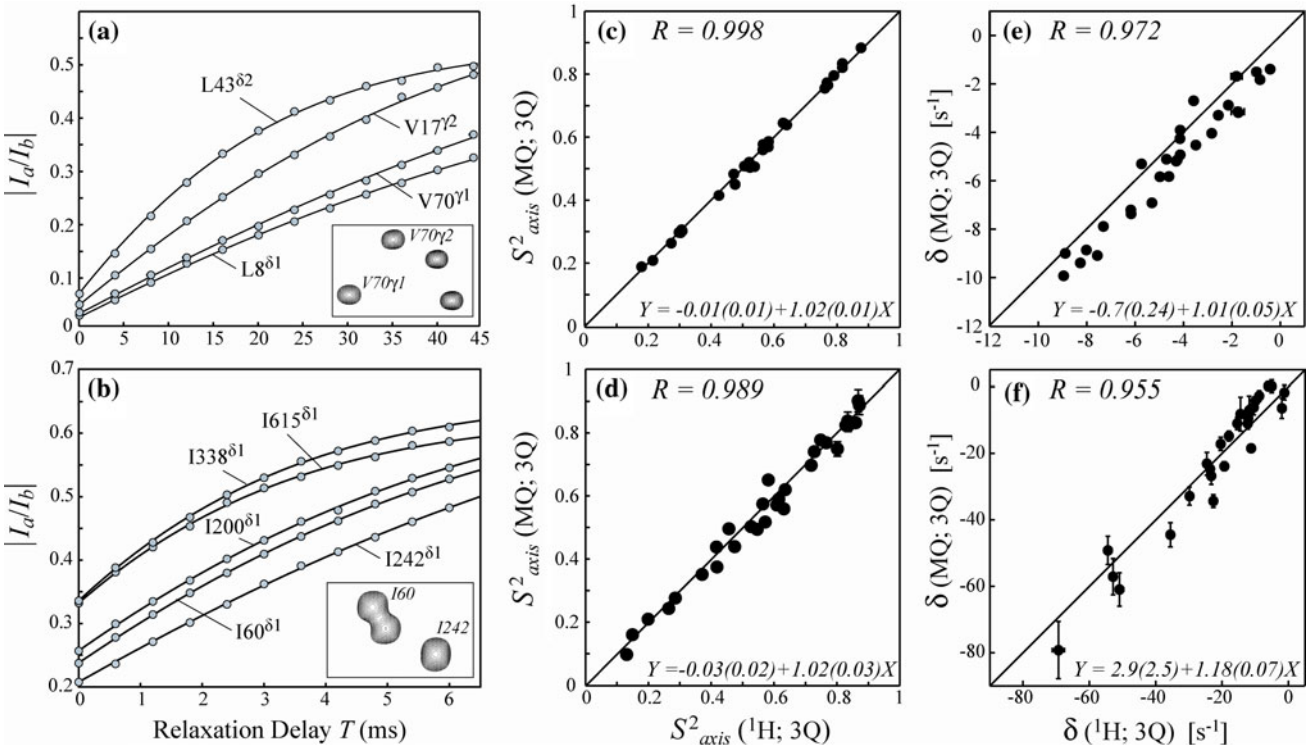

Fig. 5 Build-up curves of experimental intensity ratios, $|I_a/I_b|$, obtained using the experiment of Fig. 2 for selected methyl groups of **a** {U-[^{2}H]; Ile$^{\delta1}$-[^{13}CH$_3$]; Leu,Val-[^{13}CH$_3$, ^{12}CD$_3$]}-labeled ubiquitin (600 MHz, 10°C), and **b** {U-[^{2}H]; Ile$^{\delta1}$-[^{13}CH$_3$]}-labeled MSG (600 MHz, 37°C) best-fit to (6a). Insets in **a** and **b** show selected regions of the 'allowed' 2D spectra acquired with $T = 0$ where the peaks of at least one of the highlighted methyls of ubiquitin (**a**) and MSG (**b**) is present; **c–d** Linear correlation plots of S^2_{axis} values obtained from the measurements of η' using the experiment of Fig. 2—*y*-axis, (MQ; 3Q) versus S^2_{axis} derived from the previous measurements of ^{1}H–^{1}H cross correlation rates—*x*-axis, (^{1}H; 3Q) (Sun et al. 2011) for **c** for 29 ILV methyls of {U-[^{2}H]; Ile$^{\delta1}$-[^{13}CH$_3$]; Leu,Val-[^{13}CH$_3$,^{12}CD$_3$]}-ubiquitin, and **d** 31 methyl positions of {U-[^{2}H]; Ile$^{\delta1}$-[^{13}CH$_3$]}-MSG; **e–f** Linear correlation plots of the parameter δ (s^{-1}) from the fits of $|I_a/I_b|$ ratios obtained in the experiment of Fig. 2—*y*-axis, (MQ; 3Q)—versus δ extracted from the fits of $|I_a/I_b|$ ratios in the earlier ^{1}H–^{1}H cross-correlated relaxation measurements—*x*-axis, (^{1}H; 3Q) (Sun et al. 2011) for **e** 29 ILV methyls of ubiquitin, and **f** 31 methyl groups of {U-[^{2}H]; Ile$^{\delta1}$-[^{13}CH$_3$]}-MSG. In the MQ data-sets, S^2_{axis} values are calculated from the η' rates using (2). Best-fit parameters from a linear regression analysis of the data are shown along with Pearson correlation coefficients, *R*. Diagonal lines correspond to $y = x$

been extracted from the fits in ubiquitin and MSG, respectively. The consistency between the measures of order derived from ^{1}H relaxation in 2Q-filtered (Tugarinov et al. 2007) and 3Q-filtered (Sun et al. 2011) relaxation violated coherence transfer experiments and the values of S^2_{axis} obtained via more conventional approaches such as ^{13}C and ^{2}H relaxation, was demonstrated previously on the methyl-protonated, highly deuterated samples of 6.5-kDa protein L at 5°C, 8.5-kDa ubiquitin at 10°C, 82-kDa MSG at 37°C and 360-kDa $\alpha_7\alpha_7$ proteasome at 50°C (Sun et al. 2011; Tugarinov et al. 2007). Therefore, here we restrict our comparisons of η'-derived S^2_{axis} from the experiment in Fig. 2 (MQ; 3Q) to the values obtained from the measurements of η_{HH} via the 3Q-filtered relaxation violated coherence transfer experiments (^{1}H; 3Q; Sun et al. 2011). As shown in Fig. 5c, the S^2_{axis} values obtained for 29 methyls of ubiquitin from the η' rates are in almost ideal agreement with (^{1}H; 3Q)-derived S^2_{axis}. A good agreement between the two sets of data is also obtained for the parameter δ that accounts for cross-relaxation between the 'fast' and 'slow' coherences induced by external proton spins in (5c) (Fig. 5e). As predicted from simulations described above, the fitting of the parameter δ ($\delta < 0$ for all methyl sites) is more error-prone—it is systematically, albeit slightly, underestimated in the (MQ; 3Q) data due to residual effects of *J* evolution during the relaxation delay *T*. In fact, some residual *J* modulation of the $|I_a/I_b|$ ratios can be discerned in the upper two build-up curves in Fig. 5a for longer delays *T*.

Figure 5d illustrates the comparison between the (MQ; 3Q)-derived (η' measurements) and (^{1}H; 3Q)-derived (η_{HH} measurements) S^2_{axis} values obtained for 31 Ile$^{\delta1}$ methyls of {U-[^{2}H]; Ile$^{\delta1}$-[^{13}CH$_3$]}-MSG. The good agreement between the two sets of data indicates that the effects of *J* evolution are largely eliminated by restricting the relaxation delay *T* to the values no longer than 6 ms. Correlations of similar quality have been obtained in {U-[^{2}H]; Ile$^{\delta1}$-

[$^{13}CH_3$]; Leu,Val-[$^{13}CH_3$,$^{12}CD_3$]}-labeled MSG, although these measurements require even shorter maximal delays T ($\leq$5 ms) to eliminate the effects of incomplete J refocusing. We note that Ile$^{\delta 1}$ methyls represent a more challenging case in the 3Q-filtered relaxation violated coherence transfer experiments because of their generally longer ^{1}H T_1 relaxation times. For example, average Ile$^{\delta 1}$ ^{1}H T_1 of 1.6 s in Ile$^{\delta 1}$-{$^{13}CH_3$}-MSG was reported previously compared to 0.6 s for Leu/Val in {Ile$^{\delta 1}$-[$^{13}CH_3$], Leu, Val-[$^{13}CH_3$/$^{12}CD_3$]}-labeled sample (Tugarinov and Kay 2004b). The application of ^{1}H spin-lock followed by a 'purge' element before the start of the recycle delay in the scheme of Fig. 2 (Sun et al. 2011) equalizes the proton magnetization 'entering' the pulse scheme in each individual scan eliminating the effects of slow longitudinal ^{1}H relaxation. Finally, the correlations obtained between (MQ; 3Q) and (^{1}H; 3Q)-derived parameters δ in MSG (Fig. 5f) are notably inferior to those of ubiquitin although they remain quite high (Pearson $R > 0.95$).

In summary, we developed a relaxation violated coherence transfer NMR experiment where relaxation of MQ ^{1}H–^{13}C methyl coherences is monitored during the relaxation period. The experiment uses 3Q filtering of 'forbidden' proton transitions that has been shown recently to be optimal for relaxation violated coherence transfer measurements (Sun et al. 2011). The measurement of the sum of ^{1}H–^{1}H and ^{1}H–^{13}C cross-correlated relaxation rates in $^{13}CH_3$ methyls of methyl-protonated, highly deuterated proteins and the associated modeling of the time-dependence of the signal build-up, allow extraction of reliable measures of methyl-containing side-chain order. The described experiment is not as widely applicable as its original ^{1}H SQ relaxation-based analogue (Tugarinov et al. 2007; Sun et al. 2011). The range of its applications is clearly limited to protein systems where the fast-relaxing part of the ^{1}H magnetization has not decayed completely by the time the first relaxation point can be sampled—time-point a in the scheme of Fig. 2. It cannot be expected, therefore, that it can find applications to large proteins significantly exceeding in molecular weight the ones described in this study. Originally, the main rationale behind the described approach was based on the fact that the lines of the MQ methyl triplet are separated by the (large) value of $^1J_{CH}$. If $^1J_{CH}$ had not had to be refocused during the relaxation delay T, this would have led to reduced contributions from external proton spins, i.e. the cross-relaxation between the 'slow' and 'fast' parts of magnetization in (1) and (5a) could have been neglected. The need for as complete refocusing of J as possible, however, invalidates this 'solution'. Nevertheless, as estimated from the 2D spectra corresponding to the first time point ($T = 0$) of the 'allowed' data sets, the measurements of η' are to within $\sim$5% as sensitive as the previously published versions of the relaxation-violated coherence transfer experiments. The new scheme will serve as a valuable complement to existing NMR methodology for the measurement of side-chain order in protein molecules within $\sim$100 kDa molecular weight range.

Acknowledgments The authors thank Dr. Daoning Zhang (University of Maryland) for providing the sample of {U-[^{2}H;^{15}N]; Ile$^{\delta 1}$-[$^{13}CH_3$]; Leu,Val-[$^{13}CH_3$,$^{12}CD_3$]}-labeled human ubiquitin. The authors are grateful to Prof. Lewis E. Kay (University of Toronto, Canada) for useful and stimulating discussions.

References

Ayala I, Sounier R, Usé N, Gans P, Boisbouvier J (2009) An efficient protocol for the complete incorporation of methyl-protonated alanine in perdeuterated protein. J Biomol NMR 43:111–119

Carr HY, Purcell EM (1954) Effects of diffusion on free precession in nuclear magnetic resonance experiments. Phys Rev 94:630–638

Cho CH, Urquidi J, Singh S, Robinson GW (1999) Thermal offset viscosities of liquid H_2O, D_2O and T_2O. J Phys Chem B 103:1991–1994

Delaglio F, Grzesiek S, Vuister GW, Zhu G, Pfeifer J, Bax A (1995) NMRPipe: a multidimensional spectral processing system based on UNIX pipes. J Biomol NMR 6:277–293

Ernst RR, Bodenhausen G, Wokaun A (1987) Principles of nuclear magnetic resonance in one and two dimensions. Oxford University Press, Oxford

Gans P, Hamelin O, Sounier R, Ayala I, Durá MA, Amero CD, Noirclerc-Savoye M, Franzetti B, Plevin MJ, Boisbouvier J (2010) Stereospecific isotopic labeling of methyl groups for NMR spectroscopic studies of high-molecular-weight proteins. Angew Chem Int Ed Engl 49:1958–1962

Godoy-Ruiz R, Guo C, Tugarinov V (2010) Alanine methyl groups as NMR probes of molecular structure and dynamics in high-molecular-weight proteins. J Am Chem Soc 132:18340–18350

Howard BR, Endrizzi JA, Remington SJ (2000) Crystal structure of *Escherichia coli* malate synthase G complexed with magnesium and glyoxylate at 2.0 A resolution: mechanistic implications. Biochemistry 39:3156–3168

Ishima R, Louis JM, Torchia DA (1999) Transverse C-13 relaxation of CHD_2 methyl isotopomers to detect slow conformational changes of protein side chains. J Am Chem Soc 121:11589–11590

Ishima R, Petkova AP, Louis JM, Torchia DA (2001) Comparison of methyl rotation axis order parameters derived from model-free analyses of ^{2}H and ^{13}C longitudinal and transverse relaxation rates measured in the same protein sample. J Am Chem Soc 123:6164–6171

Kamith U, Shriver JW (1989) Characterization of the thermotropic state changes in myosin subfragment-1 and heavy meromyosin by UV difference spectroscopy. J Biol Chem 264:5586–5592

Kay LE (2011) Solution NMR spectroscopy of supra-molecular systems, why bother? A methyl-TROSY view. J Magn Reson 210:159–170

Kay LE, Prestegard JH (1987) Methyl group dynamics from relaxation of double quantum filtered NMR signals. Application to deoxycholate. J Am Chem Soc 109:3829–3835

Kay LE, Torchia DA (1991) The effects of dipolar cross-correlation on ^{13}C methyl-carbon T_1, T_2 and NOE measurements in macromolecules. J Magn Reson 95:536–547

Kay LE, Bull TE, Nicholson LK, Griesinger C, Schwalbe H, Bax A, Torchia DA (1992) The measurement of heteronuclear

transverse relaxation times in AX_3 spin systems via polarization transfer techniques. J Magn Reson 100:538–558

Korzhnev DM, Kloiber K, Kanelis V, Tugarinov V, Kay LE (2004) Probing slow dynamics in high molecular weight proteins by methyl-TROSY NMR spectroscopy: application to a 723-residue enzyme. J Am Chem Soc 126:3964–3973

Lipari G, Szabo A (1982) Model-free approach to the interpretation of nuclear magnetic relaxation in macromolecules: 2. Analysis of experimental results. J Am Chem Soc 104:4559–4570

Marion D, Ikura M, Tschudin R, Bax A (1989) Rapid recording of 2D NMR spectra without phase cycling. Application to the study of hydrogen exchange in proteins. J Magn Reson 85:393–399

Meiboom S, Gill D (1958) Modified spin-echo method for measuring nuclear relaxation times. Rev Sci Instrum 29:688

Mittermaier A, Kay LE (2002) Effect of deuteration on some structural parameters of methyl groups in proteins as evaluated by residual dipolar couplings. J Biomol NMR 23:35–45

Müller N, Bodenhausen G, Ernst RR (1987) Relaxation-induced violations of coherence transfer selection rules in nuclear magnetic resonance. J Magn Reson 75:297–334

Ollerenshaw JE, Tugarinov V, Kay LE (2003) Methyl TROSY: explanation and experimental verification. Magn Reson Chem 41:843–852

Ollerenshaw JE, Tugarinov V, Skrynnikov NR, Kay LE (2005) Comparison of $^{13}CH_3$, $^{13}CH_2D$, and $^{13}CHD_2$ methyl labeling strategies in proteins. J Biomol NMR 33:25–41

Ottiger M, Bax A (1999) How tetrahedral are methyl groups in proteins? A liquid crystal NMR study. J Am Chem Soc 121:4690–4695

Religa TL, Sprangers R, Kay LE (2010) Dynamic regulation of archaeal proteasome gate opening as studied by TROSY NMR. Science 328:98–102

Ruschak AM, Kay LE (2010) Methyl groups as probes of supramolecular structure, dynamics and function. J Biomol NMR 46:75–87

Ruschak AM, Religa TL, Breuer S, Witt S, Kay LE (2010a) The proteasome antechamber maintains substrates in an unfolded state. Nature 467:868–871

Ruschak AM, Velyvis A, Kay LE (2010b) A simple strategy for ^{13}C, ^{1}H labeling at the Ile-γ2 methyl position in highly deuterated proteins. J Biomol NMR 48:129–135

Shaka AJ, Keeler J, Frenkiel T, Freeman R (1983) An improved sequence for broadband decoupling: WALTZ-16. J Magn Reson 52:335–338

Sheppard D, Li DW, Brüschweiler R, Tugarinov V (2009) Deuterium spin probes of backbone order in proteins: a ^{2}H NMR relaxation study of deuterated carbon-α sites. J Am Chem Soc 131: 15853–15865

Sheppard D, Sprangers R, Tugarinov V (2010) Experimental approaches for NMR studies of side chain dynamics in high-molecular-weight proteins. Prog Nucl Magn Reson Spectrosc 56:1–45

Sprangers R, Kay LE (2007) Quantitative dynamics and binding studies of the 20S proteasome by NMR. Nature 445:618–622

Sprangers R, Velyvis A, Kay LE (2007) Solution NMR of supramolecular complexes: providing new insights into function. Nat Methods 4:697–703

Sun H, Kay LE, Tugarinov V (2011) An optimized relaxation-based coherence transfer NMR experiment for the measurement of side-chain order in methyl-protonated, highly deuterated proteins. J Phys Chem B 115:14878–14884

Tugarinov V, Kay LE (2004a) $^{1}H,^{13}C–^{1}H,^{1}H$ dipolar cross-correlated spin relaxation in methyl groups. J Biomol NMR 29:369–376

Tugarinov V, Kay LE (2004b) An isotope labeling strategy for methyl TROSY spectroscopy. J Biomol NMR 28:165–172

Tugarinov V, Kay LE (2005a) Methyl groups as probes of structure and dynamics in NMR studies of high-molecular-weight proteins. Chembiochem 6:1567–1577

Tugarinov V, Kay LE (2005b) Quantitative ^{13}C and ^{2}H NMR relaxation studies of the 723-residue enzyme malate synthase G reveal a dynamic binding interface. Biochemistry 44:15970–15977

Tugarinov V, Kay LE (2006a) A ^{2}H NMR relaxation experiment for the measurement of the time scale of methyl side-chain dynamics in large proteins. J Am Chem Soc 128:12484–12489

Tugarinov V, Kay LE (2006b) Relaxation rates of degenerate ^{1}H transitions in methyl groups of proteins as reporters of side-chain dynamics. J Am Chem Soc 128:7299–7308

Tugarinov V, Muhandiram R, Ayed A, Kay LE (2002) Four-dimensional NMR spectroscopy of a 723-residue protein: chemical shift assignments and secondary structure of malate synthase G. J Am Chem Soc 124:10025–10035

Tugarinov V, Hwang PM, Ollerenshaw JE, Kay LE (2003) Cross-correlated relaxation enhanced $^{1}H–^{13}C$ NMR spectroscopy of methyl groups in very high molecular weight proteins and protein complexes. J Am Chem Soc 125:10420–10428

Tugarinov V, Hwang PM, Kay LE (2004a) Nuclear magnetic resonance spectroscopy of high-molecular-weight proteins. Annu Rev Biochem 73:107–146

Tugarinov V, Sprangers R, Kay LE (2004b) Line narrowing in methyl TROSY using zero-quantum $^{1}H–^{13}C$ spectroscopy of methyl groups. J Am Chem Soc 126:4921–4925

Tugarinov V, Ollerenshaw JE, Kay LE (2005) Probing side-chain dynamics in high molecular weight proteins by deuterium NMR spin relaxation: an application to an 82-kDa enzyme. J Am Chem Soc 127:8214–8225

Tugarinov V, Kanelis V, Kay LE (2006) Isotope labeling strategies for the study of high-molecular-weight proteins by solution NMR spectroscopy. Nat Protoc 1:749–754

Tugarinov V, Sprangers R, Kay LE (2007) Probing side-chain dynamics in the proteasome by relaxation violated coherence transfer NMR spectroscopy. J Am Chem Soc 129:1743–1750

Wooten JB, Savitsky GB, Jacobus J, Beyerlein AL, Emsley JW (1979) Isotope effects on order in nematic solutions. Deuterium quadrupole coupling constants for CDH_2I. J Chem Phys 70:438–442